

Effective torsional stiffness of reinforced concrete structural walls

Da Luo^{1a}, Chaolie Ning^{2b} and Bing Li^{*3}

¹College of Civil Engineering and Architecture, Guangxi University, Nanning 530004, P.R. China

²Shanghai Institute of Disaster Prevention and Relief, Tongji University, Shanghai 200092, P.R. China

³School of Civil and Environmental Engineering, Nanyang Technological University, 639798, Singapore

(Received December 19, 2017, Revised October 18, 2018, Accepted November 22, 2018)

Abstract. When a structural wall is subjected to multi-directional ground motion, torsion-induced cracks degrade the stiffness of the wall. The effect of torsion should not be neglected. As a main lateral load resisting member, reinforced concrete (RC) structural wall has been widely studied under the combined action of bending and shear. Unfortunately, its seismic behavior under a combined action of torsion, bending and shear is rarely studied. In this study, torsional performances of the RC structural walls under the combined action is assessed from a comprehensive parametrical study. Finite element (FE) models are built and calibrated by comparing with the available experimental data. The study is then carried out to find out the critical design parameter affecting the torsional stiffness of RC structural walls, including the axial load ratio, aspect ratio, leg-thickness ratio, eccentricity of lateral force, longitudinal reinforcement ratio and transverse reinforcement ratio. Besides, to facilitate the application in practice, an empirical equation is developed to estimate the torsional stiffness of RC rectangular structural walls conveniently, which is found to agree well with the numerical results of the developed FE models.

Keywords: reinforced concrete; rectangular structural walls; finite element model; torsional stiffness

1. Introduction

Reinforced concrete (RC) structural walls are the primary lateral-load-carrying elements in many structures designed to resist earthquakes. A review of the technical literature shows considerable uncertainty with regards to the effective stiffness of these structures when subjected to seismic excitations which many design practices currently deal with by employing a stiffness reduction factor (Li and Xiang 2011, Vu *et al.* 2014). Extensive works have been conducted by various researchers over the past decades to investigate the behavior of reinforced concrete (RC) beams under pure torsion (Denis 1974, Chalioris 2006, Chiu *et al.* 2007, Lopes and Bernardo 2009, Elwan 2017) and combined loadings (Rahal and Collins 1995, Alnuaimi *et al.* 2008, Suriya *et al.* 2010, Wei *et al.* 2017), where much attention was paid to the torsional strength and stiffness, twist angle, crack patterns and failure modes of RC beams. Jakobsen (1984) conducted a series of cyclic torsional tests on reinforced concrete box members and not qualitatively described that the torsional stiffness of specimen decreased significantly after cracking, while Venkappa and Pandit (1987) found that the torsional stiffness of reinforced concrete beam declined more markedly at larger peak torsion and frequency. However, research on RC rectangular structural walls under pure torsion and

combined loading is still limited, where Peng and Wong (2011a, b) studied the behavior of RC structural walls subjected to the pure torsion and combined flexure, shear and torsion. Chena *et al.* (2016) conducted an experimental investigation on U-shaped RC thin-walls under pure torsion and then proposed a simple method to estimate the flexural cracking torque and ultimate torque. There are also limited literatures investigate the torsional stiffness of RC rectangular structural walls. To expand the knowledge regarding the contribution of torsion on the seismic behavior of RC rectangular structural walls, finite element models are built and compared with the available experimental data to demonstrate its accuracy in predicting the torque-twist angle of RC rectangular structural walls. Furthermore, the influence of axial load ratio, aspect ratio, leg-thickness ratio, eccentricity of lateral force and reinforcement details on the torsional stiffness of RC rectangular structural walls is investigated by parametrical study. Finally, to facilitate the application in practice, an empirical equation is established to predict the torsional stiffness of RC rectangle structural walls conveniently.

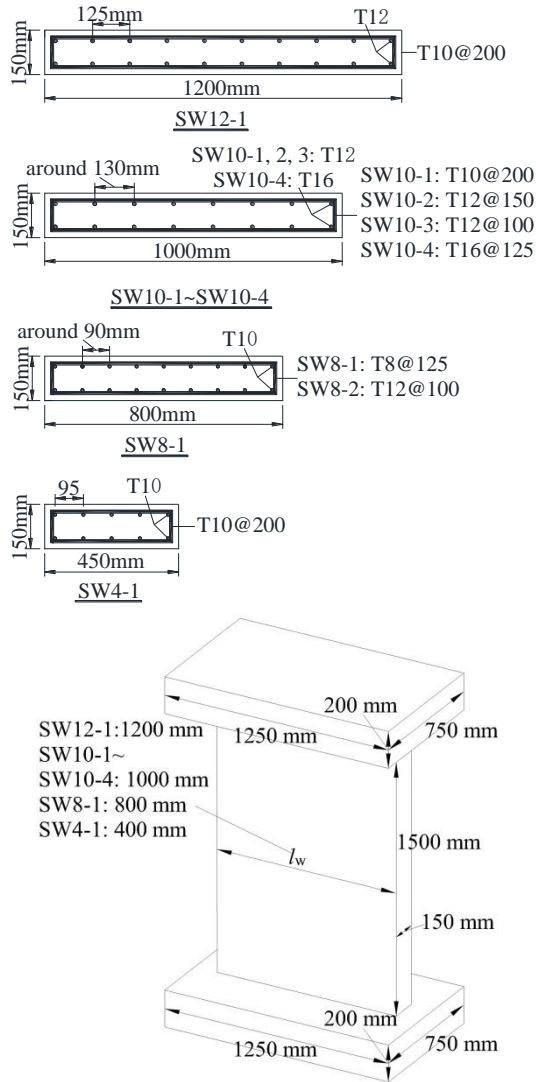
2. Experimental observations

In this section, the experimental test results of ten half-scaled RC rectangular structural walls under pure torsion and combined loading tested by Peng and Wong (2011a, b) are briefly discussed. Fig. 1 shows the dimensions and Table 1 enlists the reinforcement details of wall units. As seen from the figure, eight wall units (i.e., SW12-1, SW10-1, SW10-2, SW10-3, SW10-4, SW8-1, SW8-2 and SW4-1) are designed with the same thickness of

*Corresponding author, Associate Professor
E-mail: cbli@ntu.edu.sg

^aPh.D. Student
E-mail: luoda@gxu.edu.cn

^bAssistant Professor



Note: the dimensions and reinforcement details of SW10-100 and SW10-400 are the same as SW10-1

Fig. 1 Dimensions and reinforcement details of rectangular structural walls

150 mm, same height of 1500 mm but various depths and reinforcement details under pure torsion; while the other two wall units (i.e., SW10-100 and SW10-400) are designed with the same dimensions and reinforcement details but subjected to the lateral force acting on the top of the wall unit along with the major axis at an eccentricity of 100 mm and 400 mm, respectively. Additionally, the concrete cover depth of all the tested specimens is designed by 20 mm and the concrete compressive strength of each wall unit is determined from the average compressive strength of three 100 mm×200 mm cylinders and it listed in the last column of Table 1. Table 2 lists the properties of rebars.

Fig. 2 shows the measured torque-twist angle for the all tested specimens except SW10-1 and SW8-2 for them unanticipated damage. A detailed description about the tested setup and experimental observation for wall units under pure torsion and combined loading can be found in Peng and Wong (2011a, b).

Table 1 Reinforcement Details of Wall Units tested by Peng and Wong (2011a, b)

Units	Dimensions (mm ²)	Longitudinal Rebars	ρ_l (%)	Transverse Rebars	ρ_v (%)	ρ_{total} (%)	f_c (MPa)
SW12-1	1200×150	10T12 ² ×2	1.26	T10@200	0.55	1.81	44.2
SW10-1	1000×150	8T12 ¹ ×2	1.21	T10@200	0.55	1.76	29.5
SW10-2	1000×150	8T12 ² ×2	1.21	T12 ² @150	1.05	2.26	44.2
SW10-3	1000×150	8T12 ¹ ×2	1.21	T12 ¹ @100	1.58	2.79	29.5
SW10-4	1000×150	8T16×2	2.14	T16@125	2.23	4.37	33.8
SW8-1	800×150	9T10×2	1.18	T8@125	0.57	1.75	29.5
SW8-2	800×150	9T10×2	1.18	T12 ¹ @100	1.59	2.77	29.5
SW4-1	450×150	5T10×2	1.16	T10@200	0.58	1.74	44.2
SW10-100	1000×150	8T12 ¹ ×2	1.21	T10@200	0.55	1.76	40.2
SW10-400	1000×150	8T12 ¹ ×2	1.21	T10@200	0.55	1.76	40.2

Note: T12=deformed bar with 12 mm diameter, T12¹ and T12²=two sets of T12 rebars with different yield strengths.

Table 2 Properties of rebars

Types	Yield Strength, f_y (MPa)	Yield strain, ϵ_y (10 ⁻⁶)	Ultimate strength, f_u (MPa)
T8	433	2284	574
T10	459	2531	576
T12 ¹	499	2615	600
T12 ²	480	2828	621
T16	497	3080	605

3. Finite element model of RC structural walls

In this section, Finite Element (FE) model is built to study the torsional behavior of RC walls in Peng and Wong (2011a, b) and the comparison of experimental and numerical result are discussed herein. Then the parametrical study can be performed to investigate the torsional stiffness of RC rectangular structural walls appropriately. DIANA software is adopted in this study due to its powerful computation capability in structural analysis.

3.1 Element and materials

For concrete modeling of RC rectangular structural walls, eight node brick element (element HX24L in DIANA) is adopted for the sake of efficiency and the material properties are the same as the measured ones as enlisted in Table 2. Besides, the total strain rotating model is adopted to describe the constitutive model of concrete. As proposed by Selby and Vecchio (1993), the total strain rotating model evaluates the stress-strain relationship of concrete in principal direction of strain vector. If the principal direction of strain vector changes, the direction of concrete crack rotates accordingly. No shear transfer mechanism is accounted for by this kind of model. Moreover, the method proposed by Palermo and Collins (2003) is adopted to consider the reduction of concrete compressive strength due to concrete cracks induced by tensile strains and the increase of concrete strength and deformation due to lateral confinement. Then parabolic model which is dependent on concrete compressive fracture

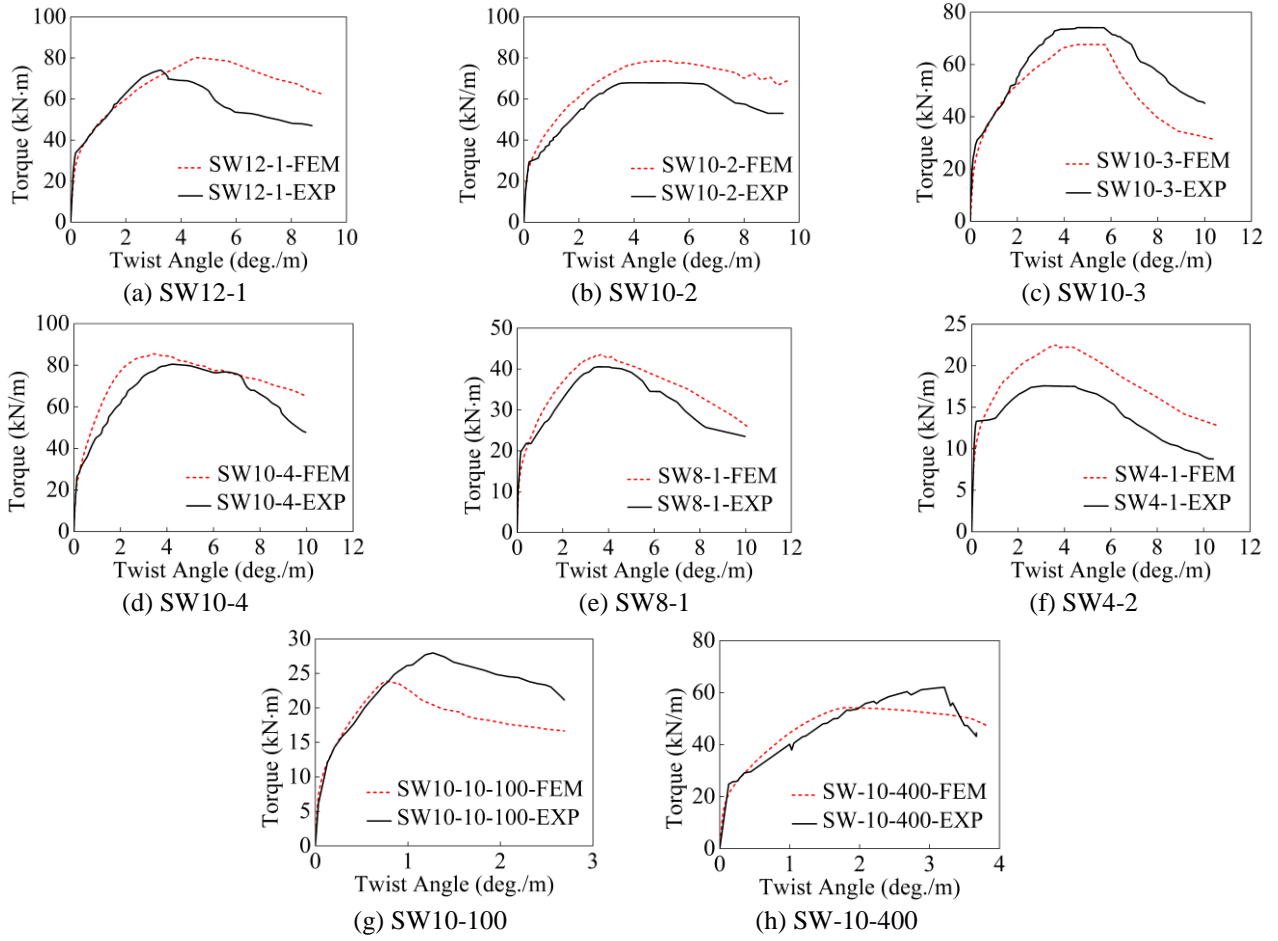


Fig. 2 Comparison of torque-twist angle curves of rectangular structural walls

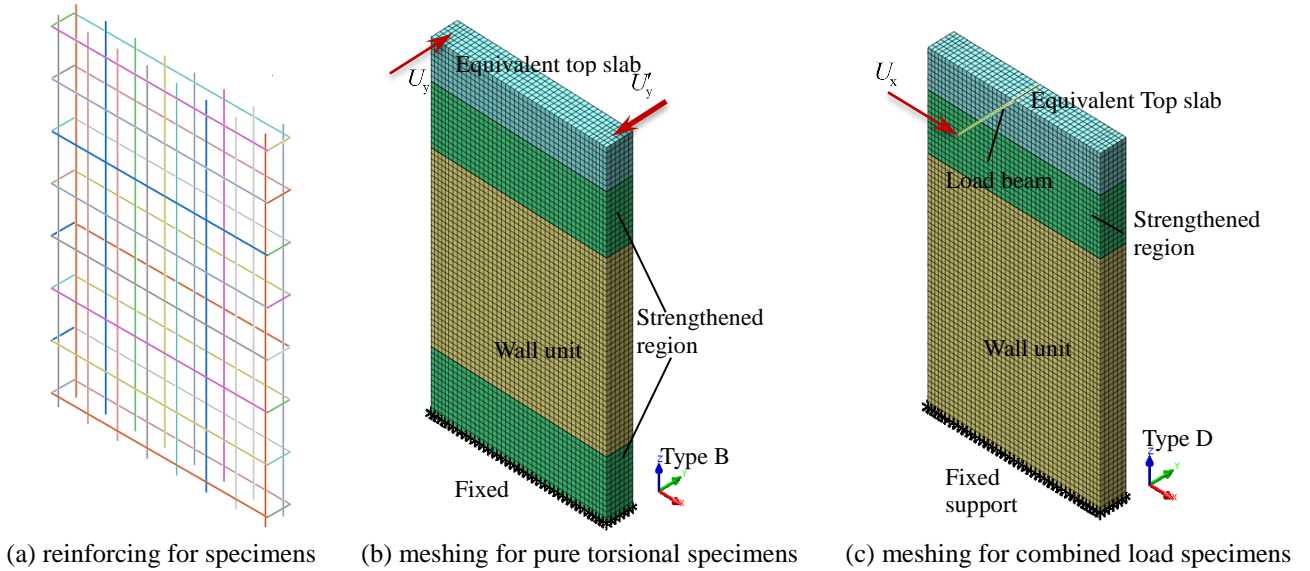


Fig. 3 Descriptions of finite element models

energy G_c and concrete compressive strength f_c is selected to describe stress-strain relationship of concrete in compression. A constant model is adopted to describe the tensile behavior of concrete and the reason is attributed to its favorable convergence after the wall unit cracks. Reinforcing bars are simulated by reinforcing bar elements

which do not have the degree of their own, the corresponding strains are computed from the so-called mother element. Therefore, a perfect bond exists between the reinforcement and surrounding concrete. Those constitutive relation had been proved efficiently and accurately in RC member numerical model by Kulkarni and

Li (2008, 2010). The reinforcing for typical wall is shown in Fig. 3(a). As for the constitutive behavior of reinforcing bars, a bilinear strain-stress relationship is adopted and the von Mises yield criterion with the isotropic strain hardening and relevant flow rule is utilized.

The FE models are built with the same geometrical dimensions and reinforcing details as the tested wall units except the slabs, while the average mesh size is 25 mm. As seen from Fig. 3(b), for the tested wall units SW10-2, SW10-3, SW10-4, SW8-1 and SW4-1 which under pure torsion, FE model is built with an equivalent top slab to assure the lateral stiffness of wall units similar to the experimental one. Then two opposite loads are applied on the top face of the top slab to produce a torque on the developed FE model. On the other hand, for specimens under combined loading, i.e., SW10-100 and SW10-400, the top slab is modeled as the same as pure torsion wall, as shown in Fig. 3(c), but a strong rigid beam is linked to the top face of the top slab at the location of the minor axis of cross section, where the rigid beam is modeled using 2-node beam elements (element L12BE in DIANA). Moreover, to prevent the stress concentration at the center point of the top slab for FE model, six nodes are assigned to link the wall element at the corresponding location. Thus, the length of the rigid beam is equal to the eccentricity plus half of the thickness of wall units. Furthermore, the lateral loads with varied eccentricities are applied at the end of the rigid beam to produce an eccentricity lateral force.

3.2 Verification of FE models

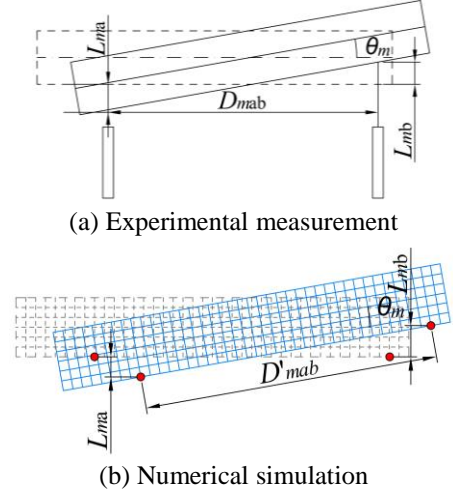
Unfortunately, in verifying the accuracy of the developed FE models, the predicted magnitude of the torque and twist angle cannot be determined from the FE model directly. The torque of FE model is similar to test, and it is calculated by the following expression

$$T = \begin{cases} F \cdot D_f & \text{For pure torsion specimens} \\ F \cdot e & \text{For combined load specimens} \end{cases} \quad (1)$$

Where F is lateral load, D_f is the distance between two load points and e is the eccentricity of lateral load. To reduce the influence of measuring positions on the predicted response of wall units, the analytical results are exported at the same locations as the experimental measurement to calculate the torque and twist angle of the selected specimens, but the expression of estimating the twist angle θ of wall units is different from the estimation using the experimental data. Specifically, as shown in Fig. 5(a), D_{mab} and D_{nab} , as defined by the distance between LVDT L_{ma} and L_{mb} , L_{na} and L_{nb} , respectively, are a constant in experimental test, so the twist angle of the specimens in test should be determined with the following expression

$$\theta = \left[\arctan\left(\frac{L_{ma} + L_{mb}}{D_{mab}}\right) - \arctan\left(\frac{L_{na} + L_{nb}}{D_{nab}}\right) \right] / D_t \quad (2)$$

Where D_t is the distance between the two measured levels. However, in numerical simulation, the displacement of wall section only can be obtained from the nodes of elements. As illustrated in Fig. 5(b), the constant distance D'_{mab} and D'_{nab} between two selected points in section m and



Note: θ_m is the measured twist angle. The dash lines represents the initial deformation and the solid line represents the torsional deformation of wall units.

Fig. 4 Method to measure the twist angle of specimens

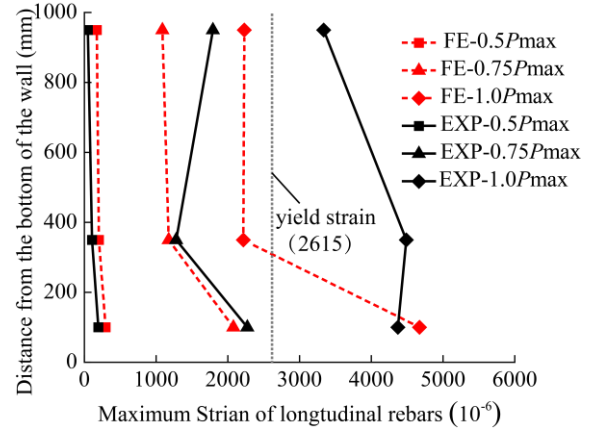


Fig. 5 Comparison of maximum strain at the same section of specimen SW10-400

n are used to predict the twist angle in numerical model

$$\theta = \left[\arcsin\left(\frac{L_{ma} + L_{mb}}{D'_{mab}}\right) - \arcsin\left(\frac{L_{na} + L_{nb}}{D'_{nab}}\right) \right] / D_t \quad (3)$$

Fig. 2 shows the predicted torque-twist angle compared to the experimental one. In general, there is a good agreement between the experimental and predicted responses. The FE model also predicts the initial stiffness, yield strength and ultimate torque accurately. However, successive deterioration of torsional stiffness can be observed during the numerical simulation, while a significant degradation of torsional stiffness occurs beyond the elastic stage when the specimen cracks in the experimental test. Nevertheless, comparison of the predicted and experimental results demonstrates that the torque versus twist angle that obtained from the developed FE model is similar to the experimental results. Fig. 5 shows the comparison of the maximum longitudinal strain of specimen SW10-400 between the experiment and numerical results. It is easy to find that the numerical model could predict the strain value well before rebar yield.

Therefore, the use of FE modeling techniques can be further extended to study the torsional behavior of RC rectangular structural walls by varying the design parameters.

3.3 Definition of torsional yield stiffness

A torsional stiffness is a very important index to study the performance of structural walls, GC is used herein to determine the torsional stiffness of structural wall, and it obtained from

$$GC = \frac{T}{\theta} \quad (4)$$

Where T is torque applied on the wall unit and θ is twist angle per unit length. A torsional yield stiffness is defined as a stiffness where the rebars first yield or the strain of concrete reached 0.002 in a RC member. Therefore, it is easy to obtain yield torsional stiffness GC_y by the above definition in a numerical model or experiment results, and it given by

$$GC_y = \frac{T_y}{\theta_y} \quad (5)$$

Where T_y is the yield torque, θ_y is the corresponding twist angle.

After that, the torsional yield stiffness ratio of RC rectangular structural walls can be determined by

$$\kappa = \frac{GC_y}{GC_i} \times 100\% \quad (6)$$

Where GC_i is the initial torsional stiffness which is the tangent stiffness at the origin.

A comprehensive parametrical study including 440 cases is carried out to investigate the influence of design parameters, for example, the axial load ratio ($\frac{N}{f_c A_g}$), aspect ratio ($\frac{h_w}{l_w}$), leg-thickness ratio ($\frac{l_w}{d_w}$), eccentricity of lateral force (e), longitudinal reinforcement ratio (ρ_l) and transverse reinforcement ratio (ρ_v) on the torsional stiffness of RC rectangular structural walls. Table 3 displays the distribution range of the investigated design parameters. Besides, similar to the experimental test, the concrete cover to outer surface of transverse reinforcement is set by 20 mm in parametrical study and the overall height of all the wall

Table 3 Design parameters investigated in parametrical study

No.	Notation	Description	Range Investigated
1	n	Axial load ratio	0, 0.05, 0.1, 0.15, 0.20
2	$\frac{h_w}{l_w}$	Aspect ratio	0.75, 1.5, 2.0, 3.0
3	$\frac{l_w}{d_w}$	Leg-thickness ratio	3.33, 5.0, 6.67
4	e	Eccentricity of lateral force (m)	0.1, 0.4, 1.0, pure torsion
5	ρ_l (%)	Longitudinal reinforcement ratio	0.54, 1.21, 2.12
6	ρ_v (%)	Transverse reinforcement ratio	0.55, 1.58

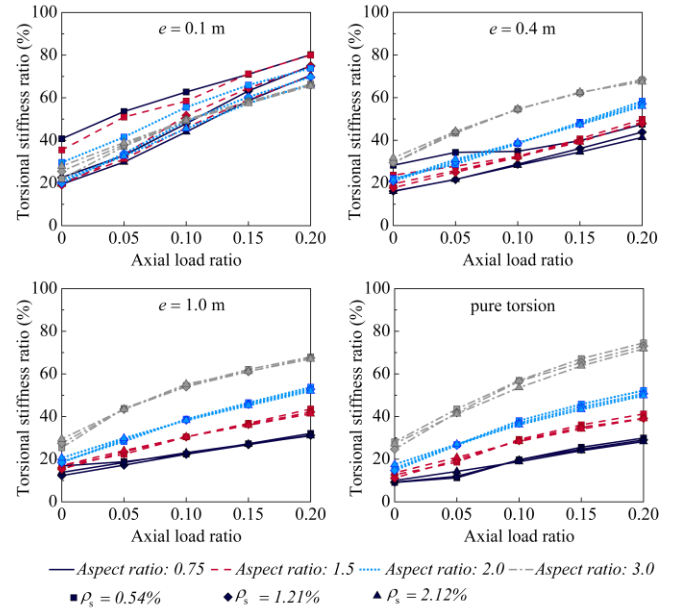


Fig. 6 Influence of axial load ratio on torsional stiffness ratios

units is designed by 1500 mm. If specimens are subjected to the axial load, the axial load should first apply on the top slab of the developed FE model and then maintained during the loading process.

3.4 parametric study

3.4.1 Influence of axial load ratio

Fig. 6 shows the influence of axial load ratio on the torsional stiffness ratio by increasing the axial load ratio from 0.0 to 0.05, 0.01, 0.15 and 0.20, respectively. As shown in the figure, the torsional stiffness ratio increases with the increase of axial load ratio under various eccentricity of lateral force, sectional dimension and reinforcement ratio. Specifically, the torsional stiffness ratio is increased by 56%, 120%, 177% and 223% approximately for walls with an eccentricity of lateral force of 0.1. Besides, for walls with an eccentricity of lateral force of 0.4, an approximate increase by 39%, 79%, 119% and 160% can be observed. Moreover, the torsional stiffness ratio is increased by 45%, 86%, 120% and 154%, respectively when walls have an eccentricity of lateral force in magnitude by 1.0 and if rectangular structural walls only enable to carry torque and axial force, the torsional stiffness ratio increases by approximate 57%, 119%, 166% and 202%, respectively. Thus, the axial load ratio plays a significant role on the torsional stiffness ratio of RC rectangular structural walls and the eccentricity of lateral force also has considerable impact on the influence of axial load ratio.

3.4.2 Influence of aspect ratio

As shown in Fig. 7, for walls with the eccentricity of lateral force in magnitude by 0.1, the torsional stiffness ratio increases slightly and approximately by 1%, 6% and 6% with the increase of aspect ratio from 0.75 to 1.5, 2.0

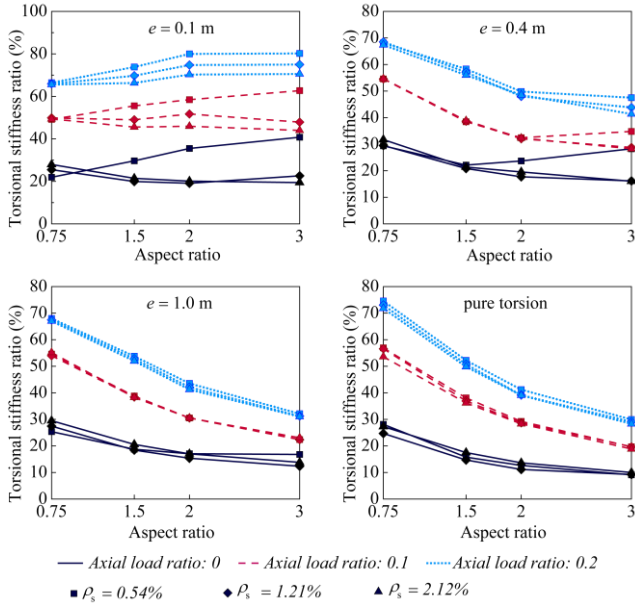


Fig. 7 Influence of aspect ratio on torsional stiffness ratios

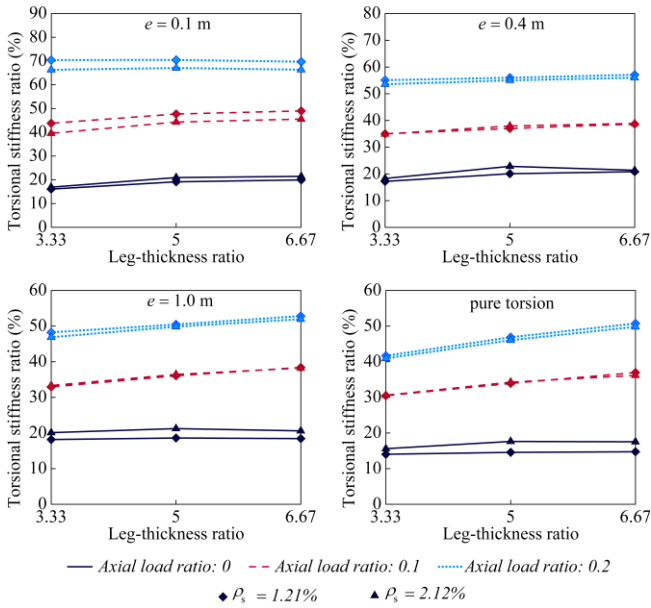


Fig. 8 Influence of leg-thickness ratio on torsional stiffness ratios

and 3.0, respectively. However, if walls are subjected to the eccentricity of lateral force of 0.4, the torsional stiffness ratio decreases by approximate 25%, 34% and 38%, respectively. Moreover, specimen only under torsion and axial load increases the torsional stiffness ratio by approximate 30%, 45%, 61%, respectively. Therefore, the influence of aspect ratio on the torsional stiffness ratio is more significant with the increase of eccentricity of lateral force. The reason can be attributed to the torque gradually dominates the external forces. In more details, compared to the wall unit with aspect ratio of 0.75, an approximate 27%, 40% and 53% reduction can be observed for walls with the aspect ratio of 1.5, 2.0, and 3.0, respectively.

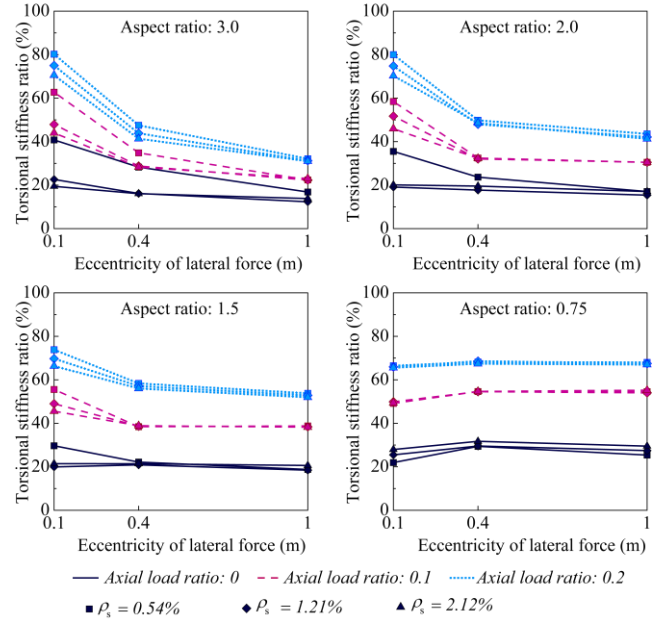


Fig. 9 Influence of eccentricity of lateral force on torsional stiffness ratios

3.4.3 Influence of leg-thickness ratio

To study the influence of leg-thickness ratio, the aspect ratio is fixed at 1.5 to diminish the influence of aspect ratio on the torsional stiffness ratio of RC rectangular structural walls. Then as seen from Fig. 8, with the increase of leg-thickness ratio from 3.3 to 5.0 and 6.7, respectively, the torsional stiffness ratio of rectangular structural walls with an eccentricity of lateral force by 0.1 increases by approximate 11% and 14%, respectively, while if walls have an eccentricity of lateral force by 0.4, the torsional stiffness ratio increases by approximate 9% and 11%, respectively. Moreover, if the eccentricity of lateral force of walls becomes 1.0, an approximate increase by 8% and 11% can be observed. Additionally, when the leg-thickness ratio increases by 50% and 100% for walls only subjected to torsion and axial load, there is an increase in torsional stiffness ratio by approximate 11% and 16%, respectively. Therefore, with the increase of leg-thickness ratio, the torsional stiffness ratio has a trifling uptrend, where the eccentricity of lateral force has bare impact on the influence of leg-thickness ratio.

3.4.4 Influence of eccentricity of lateral force

The influence of eccentricity of lateral force is indicated in Fig. 9. As seen from the figure, all the torsional stiffness ratios except the wall units with aspect ratio 0.75 show a decrease trend with the increase of eccentricity of lateral force. Specifically, there is an approximate 35% and 50% reduction on the torsional stiffness ratio for walls with the aspect ratio of 3.0 if the eccentricity of lateral force increases from 0.1 to 0.4 and 1.0, respectively. If the aspect ratio of RC rectangular structural walls becomes 2.0, the torsional stiffness ratio diminishes by approximate 29% and 37%, respectively. For walls with the aspect ratio of 1.5, the stiffness ratio decreases by approximate 16% and 20%,

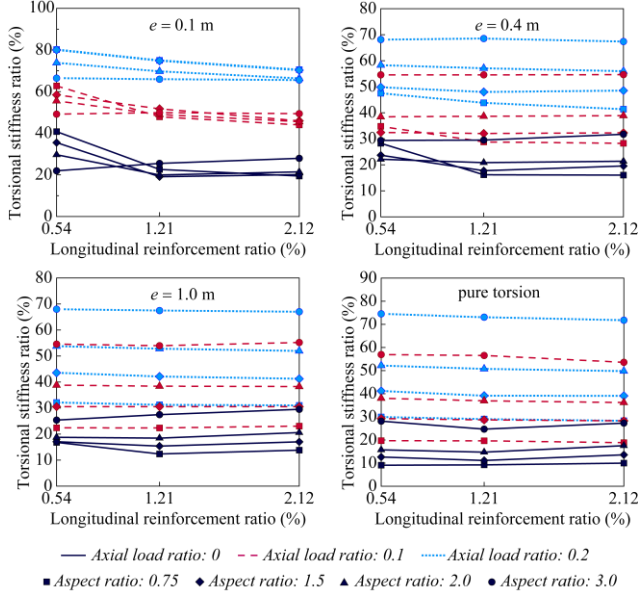
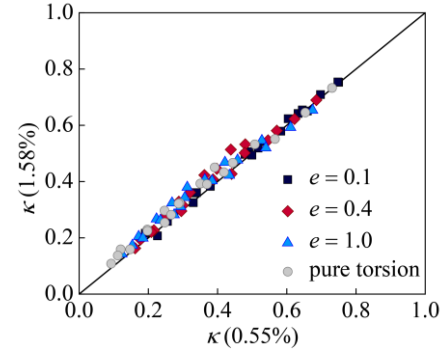


Fig. 10 Influence of longitudinal reinforcement ratio on torsional stiffness ratios

respectively. However, if the aspect ratio of walls decreases to 0.75, the influence of eccentricity of lateral force on the torsional stiffness ratio is different. As depicted in the last graph of Fig. 9, the torsional stiffness ratio of walls increases by approximate 11% and 8%, respectively with an increase of eccentricity of lateral force from 0.1 to 0.4 and 1.0, which indicates that the influence of aspect ratio on the eccentricity of lateral force is significant. Additionally, as compared by the blue lines and green lines in Fig. 9, the longitudinal reinforcement ratio has certain effects on the influence of eccentricity of lateral force when the longitudinal reinforcement ratio of RC rectangular structural walls is designed by 1.21% and 0.54%, respectively. With the decrease of axial load ratio, the influence of longitudinal reinforcement ratio on the eccentricity of lateral force can be more serious. However, if the magnitude of longitudinal reinforcement ratio is larger than 1.21%, there is minimal effect on the influence of eccentricity of lateral force on the torsional stiffness ratio of rectangular structural walls. On the other hand, the transverse reinforcement ratio only has slight impact to the influence of eccentricity of lateral force on the torsional stiffness ratio of rectangular structural walls when it changes from 0.55% to 1.58%.

3.4.5 Influence of longitudinal reinforcement ratio

As shown in Fig. 10, the influence of longitudinal reinforcement ratio on the torsional stiffness ratio becomes less significant with the increase of eccentricity of lateral force. Specifically, when the longitudinal reinforcement ratio increases from 0.54% to 1.21% and 2.12%, an approximate decrease by 14% and 17% can be observed for walls under an eccentricity of lateral force of 0.1, while for walls with the eccentricity of lateral force of 0.4, a rough decrease by 8% and 7% can be observed. When the eccentricity of lateral force is larger than 1.0, the torsional stiffness ratio is roughly the same, regardless of walls with



Note: $\kappa(1.58\%)$ indicates the torsional stiffness with transverse reinforcement ratio 1.58%, while $\kappa(0.55\%)$ indicates the torsional stiffness with transverse reinforcement ratio 0.55%

Fig. 11 Influence of transverse reinforcement ratio on torsional stiffness ratios

the magnitude of axial load ratios. Besides, the aspect ratio has certain impact on the influence of longitudinal reinforcement ratio on the torsional stiffness ratio when the eccentricity of lateral force is less than 0.4.

3.4.6 Influence of transverse reinforcement ratio

The comparison of the torsional stiffness ratio between transverse reinforcement ratio 0.55% and 1.58% is presented in Fig. 11. As seen from the figure, the maximum increase in torsional stiffness only is 11%, when the transverse reinforcement ratio changed from 0.55% to 1.58%.

4. Development of empirical equation

Based on the above results, the torsional stiffness ratio of RC rectangular structural walls should increase with the increase of axial load ratio. The influence of aspect ratio and eccentricity of lateral force on the torsional stiffness ratio is also obvious. Similarly, there is a significant influence of longitudinal reinforcement ratio on the torsional stiffness ratio of RC rectangular structural walls. However, the influence of transverse reinforcement ratio and leg-thickness ratio on the torsional stiffness ratio is slight. Therefore, an empirical equation is proposed in this section to evaluate the torsional stiffness ratio of RC rectangular structural walls as follows

$$\kappa = 2.36n + (0.0075 - 0.038n) \left(2.77 \frac{l_w}{h_w} + 4.12 \right) + (1.65n + 0.082) \left(\frac{0.022}{e + 0.05} - 0.093 \right) \left(3.8 \frac{h_w}{l_w} - 2.56 \right) + 0.01 \frac{l_w}{d_w} + \lambda_l + \lambda_v \quad (7)$$

with $\lambda_l = (0.3n - 0.1) \left(\frac{0.13}{e + 0.05} + 0.06 \right)$
 $\left(0.006 \frac{l_w}{h_w} - 0.005 \right) \left(\frac{0.7}{\rho_l} - \frac{0.01}{\rho_l^2} \right)$, $\lambda_v = 1.86\rho_v$
 λ_l is a parameter to represent the influence of longitudinal reinforcement ratio, while λ_v is a parameter to represent the influence of transverse reinforcement ratio.

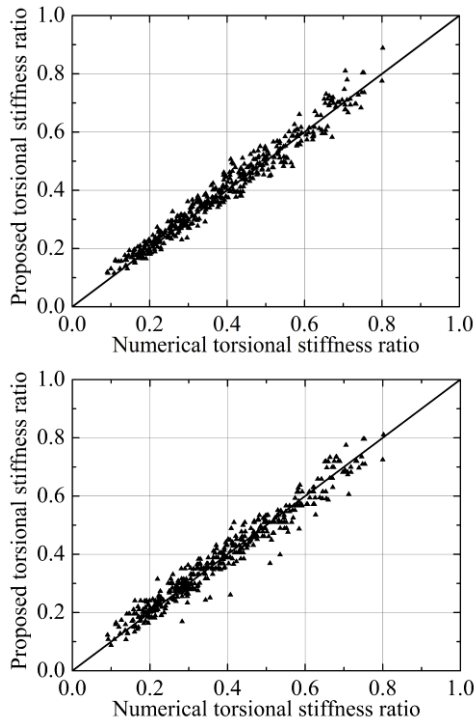


Fig. 12 Comparison of torsional stiffness ratio between prediction by empirical formula and numerical simulation

Fig. 12(a) illustrates the comparison of torsional stiffness ratio between the prediction by Eq. (7) and numerical simulation by the developed FE models. Apparently, the proposed empirical equation predicts the torsional stiffness ratio of RC rectangular structural walls accurately.

The above studies show that the influence of transverse reinforcement ratio and leg-thickness ratio on the torsional stiffness ratio is limited, therefore, a simplified equation which ignore the transverse reinforcement ratio and leg-thickness ratio could be proposed,

$$\kappa = 1.63n + (0.25n + 0.1) \left(1.24 \frac{l_w}{h_w} + 0.2 \right) + (n + 0.072) \left(\frac{0.1}{e + 0.05} - 0.33 \right) \left(1.28 \frac{h_w}{l_w} - 0.97 \right) - 2.25\rho_l + 0.14 \quad (8)$$

It is clearly observed in Fig. 12(b) that the simplified empirical equation also predicts the torsional stiffness ratio well.

5. Conclusions

An approach assessing the torsional stiffness of RC structural walls is proposed in this paper, a parametrical investigation comprising 440 cases is conducted. The follow conclusions can be drawn.

- With the axial load ratio increasing from 0 to 0.2, the torsional stiffness increases roughly 154~223%.
- The influence of aspect ratio on the torsional stiffness ratio is most significant when the eccentricity of lateral

force is larger than 0.4. Roughly a 38~61% increase is obtained with the aspect ratio change from 0.75 to 3.0. As the aspect ratio increases, walls with larger eccentricity of lateral force and less axial load ratio decrease the torsional stiffness ratio more significantly. However, when the aspect ratio is larger than 0.75, the torsional stiffness ratio inversely correlated with an increase of eccentricity of lateral force, with an increasing about 20~50%. Additionally, if the aspect ratio is less than 0.75, the eccentricity of lateral force has slight impact on the torsional stiffness ratio.

- The longitudinal reinforcement ratio has a significant influence on the torsional stiffness ratio only when the specimen has larger aspect ratio, lower axial load ratio and lower eccentricity of later force, which roughly decreases 17% when the longitudinal reinforcement ratio rises from 0.54% to 2.12%. On the other hand, the torsional stiffness ratio only increases approximately 10% when the Transverse reinforcement ratio changes from 0.55% to 1.58%.

- A simplified empirical equation is finally proposed to evaluate the torsional stiffness ratio of RC rectangular structural walls, which is found to agree well with the numerical results predicted by the developed FE models.

References

- Alnuaimi, A.S., Khalifa, S.A.J. and Abdelwahid, H. (2008), "Comparison between solid and hollow reinforced concrete beams", *Mater. Struct.*, **41**(1), 269-286.
- Chena, S., Diaoab, B., Guo, Q., Cheng, S.H. and Ye, Y. (2016), "Experiments and calculation of U-shaped thin-walled RC members under pure torsion", *Eng. Struct.*, **106**(1), 1-14.
- Chiu, H.J., Fang, I.K., Young, W.T. and Shiau, J.K. (2007), "Behavior of reinforced concrete beams with minimum torsional reinforcement", *Eng. Struct.*, **29**(9), 2193-2205.
- Denis, M. (1974), "The behavior of structural concrete beams in pure torsion", Ph.D. Dissertation, University of Toronto, Ontario, Canada.
- Elwan, S.K. (2017), "Torsion strengthening of RC beams using CFRP (parametric study)", *KSCCE J. Civil Eng.*, **21**(4), 1273-1281.
- Jakobsen, B., Hjorth-Hansen, E. and Holand, I. (1984), "Cyclic torsion tests of concrete box columns", *J. Struct. Eng.*, **110**(4), 803-822.
- Kulkarni, S.A. and Li, B. (2008), "Finite element analysis of precast hybrid-steel concrete connections under cyclic loading", *J. Constr. Steel Res.*, **64**(2), 190-201.
- Li, B. and Kulkarni, S.A. (2010), "Seismic behaviour of reinforced concrete exterior wide beam-column joints", *ASCE J. Struct. Eng.*, **136**(1), 26-36.
- Li, B. and Xiang, W.Z. (2011), "Effective Stiffness of Squat Structural Walls", *ASCE J. Struct. Eng.*, **137**(12), 1470-1479.
- Lopes, S.M.R. and Bernardo, L.F.A. (2009), "Twist behavior of high-strength concrete hollow beams-Formation of plastic hinges along the length", *Eng. Struct.*, **31**(1), 138-149.
- Palermo, D. and Vecchio, F.J. (2003), "Compression field modeling of reinforced concrete subjected to reversed loading: formulation", *ACI Struct. J.*, **100**(5), 616-625.
- Peng, X.N. and Wong, Y.L.W. (2011a), "Experimental study on reinforced concrete walls under combined flexure, shear and torsion", *Mag. Concrete Res.*, **63**(6), 459-471.
- Peng, X.N. and Wong Y.L.W. (2011b), "Behavior of reinforced

- concrete walls subjected to monotonic pure torsion-an experimental study”, *Eng. Struct.*, **33**(9), 2495-2508.
- Rahal, K.N. and Collins, M.P. (1995), “Effect of thickness of concrete cover on shear-torsion interaction-an experimental investigation”, *ACI Struct. J.*, **92**(3), 334-342.
- Selby, R.G. and Vecchio, F.J. (1993), “Three-dimensional constitutive relations for reinforced concrete”, Report No. 93-02, Department of Civil Engineering, University of Toronto, Toronto, Canada.
- Suriya, P., Belarbi, A. and You, Y.M. (2010), “Seismic performance of circular RC columns subjected to axial force, bending, and torsion with low and moderate shear”, *Eng. Struct.*, **31**(1), 46-59.
- Venkappa, V. and Pandit G.S. (1987), “Cyclic torsion tests on reinforced concrete beams”, *J. Struct. Eng.*, **113**(6), 1329-1340.
- Vu, N.S., Li, B. and Beyer, K. (2014), “Effective stiffness of reinforced concrete coupling beams”, *Eng. Struct.*, **76**(1), 371-382.
- Wei, H.S., Yu, Z.K. and Jie, W.C. (2017), “The bending-shear-torsion performance of prestressed composite box beam”, *Struct. Eng. Mech.*, **62**(5), 577-585.

KT